# Development and application of the moments method transport analysis to plasma flows in 3D configurations

D. A. Spong*, J. H. Harris*, A. S. Ware+, S. P. Hirshman*, L. A. Berry*
**Oak Ridge National Laboratory, Oak Ridge, Tennessee 37831 U.S.A.*
*+University of Montana-Missoula, Missoula, Montana 59812 U.S.A.*

Shearing rates of neoclassical flows can attain levels that are relevant to turbulence suppression. Stellarators offer several options for the control and generation of such flows. First, configuration selection and profile control can lead to transport barrier formation, as has been demonstrated recently in the LHD (Large Helical device) experiment. Second, the nonlinear nature of the ambipolar electric field condition results in regimes where multiple roots can exist. Near points where these roots merge/bifurcate, weak changes in plasma parameters can result in large increases in E × B shearing rates. Such regimes have been found particularly in the case of the QPS compact quasi-poloidal stellarator and are analyzed here.

Keywords: moments method, E × B shear, sheared flow, neoclassical, ambipolar, momentum conservation. stellarator.

## 1. Introduction

A moments transport method has been developed for stellarators [1] that predicts the three-dimensional variation of the neoclassical plasma flow velocity over the plasma volume; in addition, the self-consistent ambipolar electric field, particle and energy fluxes are calculated. In previous applications of this model [2], we have examined the shearing rates of poloidal flow velocity components over a range of different stellarator devices, indicating a significant dependence on magnetic configuration. These velocity components include mixtures of perpendicular (E × B) and parallel (neoclassical, Pfirsch-Schlüter) flows. While shearing of parallel velocities can be expected to have an impact on finite $k_{||}$ turbulence and nonlinear MHD, drift wave turbulence suppression is thought to be most strongly influenced by shearing in the E × B flows. For this reason, in this paper, the moments analysis is extended to calculate E × B shearing rates and to search for regimes where this type of flow shearing can be enhanced.

## 2. Equations

A code (PENTA) has been developed that solves the moment equations derived in Ref. [3] for arbitrary stellarator configurations. The basic equations are the parallel momentum balance coupled with the perpendicular particle and energy transport equations.

$$\begin{bmatrix} \mathcal{M}_i + \Lambda_{ii} & \frac{\tau_{ii}}{m_i n_i}\Lambda_{ie} \\ \Lambda_{ei} & \mathcal{M}_e + \Lambda_{ee} \end{bmatrix} \begin{bmatrix} U_i \\ Q_i \\ U_e \\ Q_e \end{bmatrix} = -\begin{bmatrix} \mathcal{N}_i & 0 \\ 0 & \mathcal{N}_e \end{bmatrix} \begin{bmatrix} X_{i1} \\ X_{i2} \\ X_{e1} \\ X_{e2} \end{bmatrix} \quad (1)$$

$$\begin{bmatrix} \Gamma_i \\ q_i / T_i \\ \Gamma_e \\ q_e / T_e \end{bmatrix} = \begin{bmatrix} \frac{n_i m_i}{\tau_{ii}\langle B^2 \rangle}\mathcal{N}_i & 0 \\ 0 & \frac{n_e m_e}{\tau_{ee}\langle B^2 \rangle}\mathcal{N}_e \end{bmatrix} \begin{bmatrix} U_i \\ Q_i \\ U_e \\ Q_e \end{bmatrix} + \begin{bmatrix} \mathcal{L}_i & 0 \\ 0 & \mathcal{L}_e \end{bmatrix} \begin{bmatrix} X_{i1} \\ X_{i2} \\ X_{e1} \\ X_{e2} \end{bmatrix} \quad (2)$$

These are given in equations (1) and (2) where

$$U_a = \langle B u_{||a} \rangle,\ Q_a = \frac{2}{5p_a}\langle B q_{||a} \rangle,\ X_{a1} = -\frac{1}{n_a}\frac{dp_a}{ds} - e_a\frac{d\phi}{ds},\ X_{a2} = -\frac{dT_a}{ds}$$

$$\Lambda_{ii} = -\frac{\tau_{ii}}{n_i m_i}\begin{bmatrix} \ell_{11}^{ii} & -\ell_{12}^{ii} \\ -\ell_{21}^{ii} & \ell_{22}^{ii} \end{bmatrix} \simeq \begin{bmatrix} 0 & 0 \\ 0 & \sqrt{2} \end{bmatrix};\quad \Lambda_{ee} = -\frac{Z\tau_{ee}}{n_e m_e}\begin{bmatrix} \ell_{11}^{ee} & -\ell_{12}^{ee} \\ -\ell_{21}^{ee} & \ell_{22}^{ee} \end{bmatrix} \simeq \begin{bmatrix} Z & -\frac{3}{2}Z \\ -\frac{3}{2}Z & \sqrt{2}+\frac{13}{4}Z \end{bmatrix}$$

$$\Lambda_{ei} = -\frac{Zn_i}{n_e}\frac{\tau_{ee}}{\tau_{ei}}\begin{bmatrix} 1 & 0 \\ -\frac{3}{2} & 0 \end{bmatrix};\quad \Lambda_{ie} = -\frac{Zn_i m_e}{\tau_{ei}}\begin{bmatrix} 1 & -\frac{3}{2} \\ 0 & 0 \end{bmatrix};$$

and other quantities are as defined in Ref. [3]. The neoclassical transport coefficients/viscosities $\mathcal{M}_{i,e}$, $\mathcal{L}_{i,e}$, $\mathcal{N}_{i,e}$ have been expressed in terms of velocity integrals over mono-energetic coefficients that are computed by the DKES code [4]. In order to provide a database for these

*author's e-mail: spongda@ornl.gov*

calculations, DKES is run for a range of flux surfaces, collisionalities and electric field values.

## 3. High E × B shearing regime in QPS

The QPS is a compact (<R>/<a> = 2.7), low rotational transform ($\iota$ = 0.15 to 0.3) configuration with approximate quasi-poloidal symmetry and low effective ripple ($\varepsilon^{3/2} \sim 10^{-4}$ to $7\times10^{-3}$). This form of quasi-symmetry allows low effective levels of poloidal viscosity and higher poloidal flow velocities than other configurations. The combination of low transform and near poloidal symmetry results in better alignment between the ambiently-driven ⊥ flows (E × B and diamagnetic) and the direction of minimum gradients in |B|, leading to lowered magnetic pumping for such flows. This is reflected in smaller off-diagonal stress tensor components and less conversion of ⊥ flows to ∥ flows.

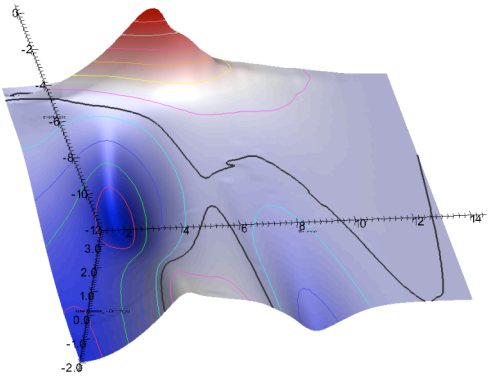

Fig 1(a) Elevation plot of $\Gamma_{ion}$-$\Gamma_{elec}$ vs. e<a>$E_r/kT_e$ and <r>/<a> for n(0) = $7 \times 10^{19}$ $m^{-3}$.

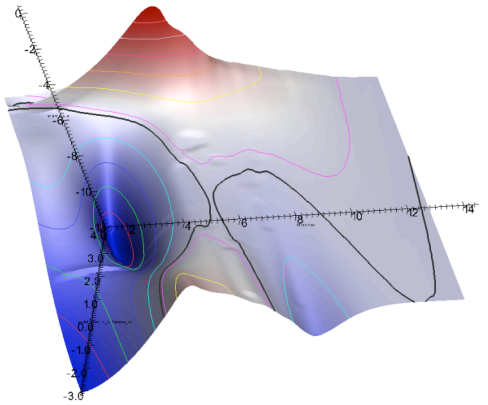

Fig 1(b) Elevation plot of $\Gamma_{ion}$-$\Gamma_{elec}$ vs. e<a>$E_r/kT_e$ and <r>/<a> for n(0) = $10^{20}$ $m^{-3}$ (solid black contour lines represent parameters for which $\Gamma_{ion}$-$\Gamma_{elec}$ = 0.

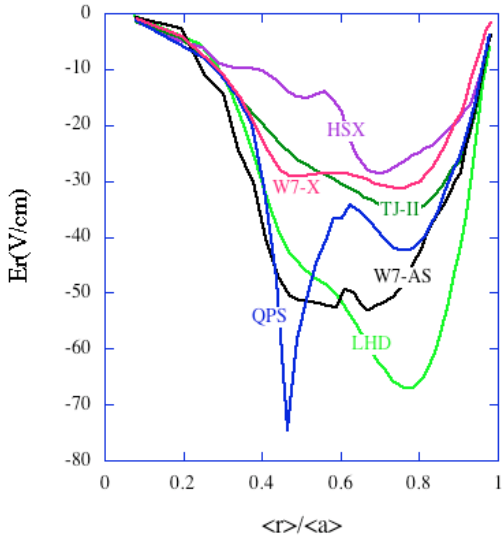


Fig. 2 Ambipolar electric field profiles for a range of configurations. All devices are scaled to <B> = 1 Tesla and <a> = 0.32 m.

From the perspective of the ambipolar transport condition (when properly coupled to neoclassical viscous effects) these characteristics can lead to the existence of additional ambipolar roots beyond the usual ion and electron solutions that are known for the case of transport models of simplified stellarators with limited helicities. An example of this characteristic is shown in Fig. 1.

As indicated, for these parameters and profiles [here $T_e(0) = T_i(0) = 0.6$ keV], the two ambipolar contours begin to merge/cross as the density is increased. This leads to a region of very high E × B shearing that could provide the basis for internal transport barrier formation.

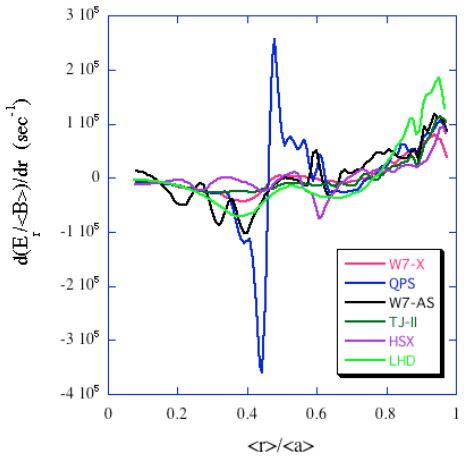


Fig. 3 E × B shearing rates for different configurations.

From limited surveys, such root merging, leading to high shearing rates has been found to be more prevalent in

QPS than other configurations. In Fig. 2, ambipolar electric field profiles are plotted for the same profiles and parameters for a range of devices. The associated E × B shearing rates are plotted in Fig. 3. In order to suppress drift turbulence, a simplified criterion is that such shearing levels need to be similar to drift wave growth rates. As analyzed in Ref. [5] for a variety of stellarators, typical growth rates range from 0.5 to 1.1 × $10^5$ $sec^{-1}$ for QPS (albeit based on different parameters and profiles than used here). The QPS shearing rates shown in Fig. 3 exceed these levels near the edge and <r>/<a> = 0.4 to 0.

## 4. E × B shearing in LHD SDC regime

A recent experimental achievement of substantial interest has been the generation of super dense core (SDC) plasmas in the LHD device [6] with low recycling and high density gradient internal diffusion barriers. This regime has been accessed by pellet injection and potentially offers extrapolation to high density/low temperature ignition scenarios. In a previous analysis of neoclassical flows in this regime, the moments model of this paper was applied to LHD, using an assumed sequence of increasingly peaked density profiles. This analysis has now been extended to examine a sequence of different equilibria with varying magnetic axis location and flux surface shaping. The highest levels of E × B shearing have been found either for equilibria with large axis shifts or those with oblate flux surface shapes at the ζ = 0 plane. An example of shearing rates in the E × B velocity and contra-variant poloidal ion flow velocity are shown in Fig. 4. Results from a sequence of profiles are displayed here, starting with a broad density profile with $n(0) = 6 \times 10^{19}$ $m^{-3}$ (red curve) and progressing to a very peaked density profile with $n(0) = 4.5 \times 10^{20}$ $m^{-3}$ (magenta curve). While these shearing levels do not quite reach levels that might be expected to form transport barriers, they could provide a background level that could supplement self-regulating turbulence-generated zonal flows.

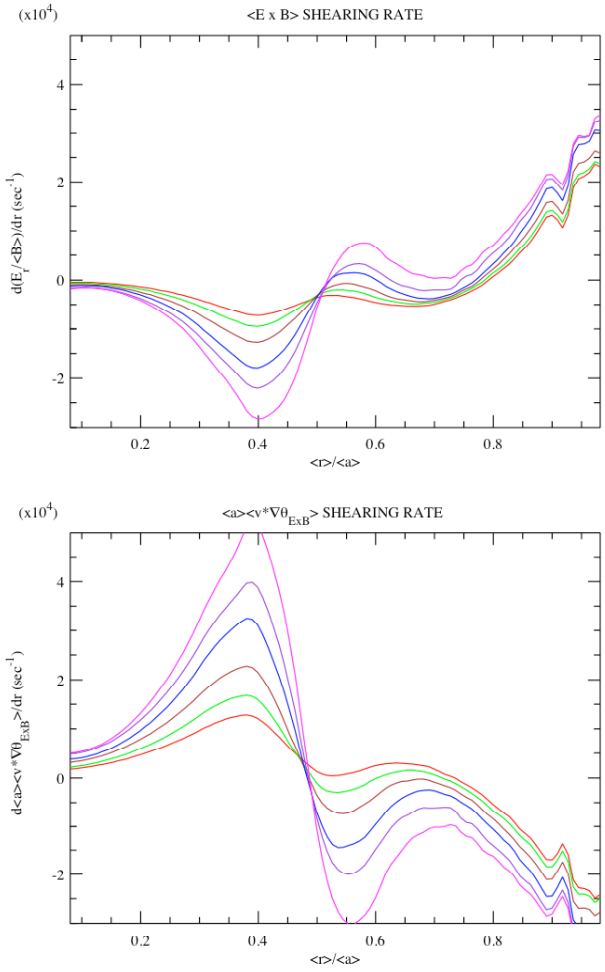


Fig. 4 E × B shearing rates and poloidal flow shearing rates for an outward shifted LHD equilibrium with $R_0$ = 3.8 m.

## 5. QPS flexibility at reduced magnetic field levels

If QPS is operated at reduced magnetic field levels in the range of <B> = 0.3 Tesla, the planar toroidal magnetic field coils have enough current capacity to introduce QP-symmetry breaking effects. These effects were analyzed previously in Ref. [2]. They have been re-analyzed with the current version of the PENTA code with respect to E × B shearing levels. As indicated in Fig. 5, variations in these coil currents can significantly modify the effective ripple [7] coefficient.

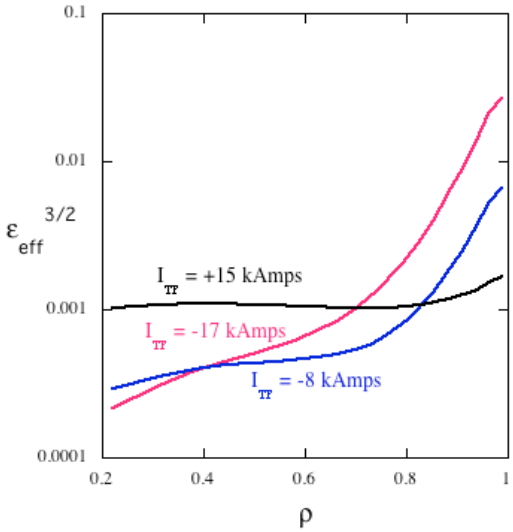


Fig. 5 – Effective ripple coefficient for low field QPS operation (<B> = 0.3 T) as a function of planar toroidal field current level.

Such variations in ripple levels lead to a range of different electric field levels, as are shown in Fig. 6. These lead to the differing E × B shearing levels that are shown in Fig. 7. As can be seen, in the <r>/<a> = 0.4 to 0.5 range, the cases with the higher effective ripple level tends to have lower shearing levels, while the cases with the lower effective ripple have higher shearing levels. This type of configuration change is thus expected to

provide useful tests of the effects of different E × B shearing levels.

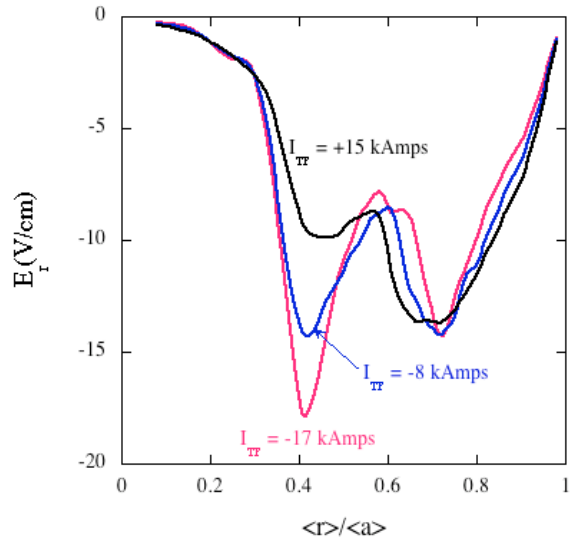


Fig. 6 Ambipolar electric field profiles vs. radius and toroidal planar coil current.

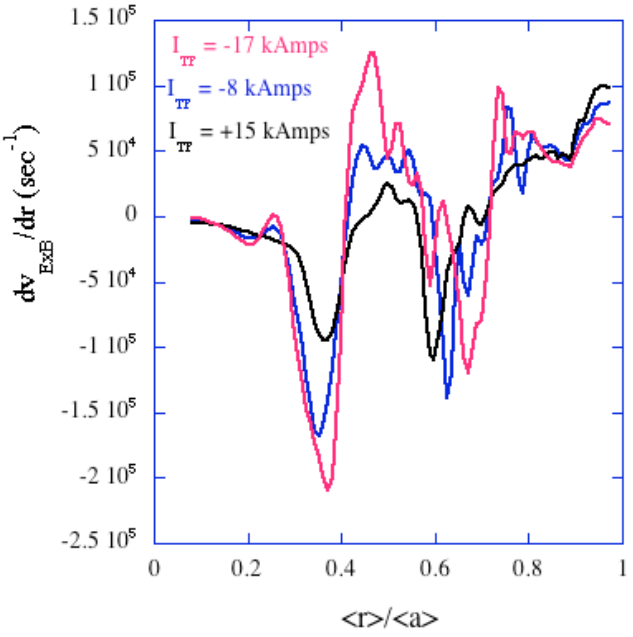


Fig. 7 E × B shearing levels vs. radius and toroidal planar coil current.

## References

[1] D. Spong, Fusion Science and Tech. **50** (2006) 343.
[2] D. Spong, et al., Nuclear Fusion **47** (2007) 626.
[3] H. Sugama, S. Nishimura, Phys. of Plasmas 9 (2002) 4637.
[4] W. I. Van Rij, S. P. Hirshman, Phys. Fluids **B1** (1989) 563.
[5] G. Rewoldt, et al., Phys. of Plasmas **12** (2005) 1047.
[6] N. Ohyabu, et al., Phys. Rev. Lett. **97** (2006) 055002-1.
[7] V. V. Nemov, et al., Phys. of Plasmas 6 (1999) 4622.

*author's e-mail: spongda@ornl.gov*